the plant journal

SEB Society for Experimental Biology

The Plant Journal (2018) **96,** 748–760 doi: 10.1111/tpj.14065

Hybridization-facilitated genome merger and repeated chromosome fusion after 8 million years

Terezie Mandáková[1], Xinyi Guo[1], Barış Özüdoğru[2], Klaus Mummenhoff[3] and Martin A. Lysak[1,*]

[1]*CEITEC – Central European Institute of Technology, Masaryk University, 625 00 Brno, Czech Republic,*

[2]*Department of Biology, Faculty of Science, Hacettepe University, 06800 Beytepe, Ankara, Turkey, and*

[3]*Department of Biology/Botany, University of Osnabrück, Barbarastraße 11, 49076, Osnabrück, Germany*

Received 22 June 2018; revised 1 August 2018; accepted 6 August 2018; published online 12 August 2018.

*For correspondence (e-mail martin.lysak@ceitec.muni.cz).

SUMMARY

The small genus *Ricotia* (nine species, Brassicaceae) is confined to the eastern Mediterranean. By comparative chromosome painting and a dated multi-gene chloroplast phylogeny, we reconstructed the origin and subsequent evolution of *Ricotia*. The ancestral *Ricotia* genome originated through hybridization between two older genomes with $n = 7$ and $n = 8$ chromosomes, respectively, on the Turkish mainland during the Early Miocene (*c.* 17.8 million years ago, Ma). Since then, the allotetraploid ($n = 15$) genome has been altered by two independent descending dysploidies (DD) to $n = 14$ in *Ricotia aucheri* and the Tenuifolia clade (2 spp.). By the Late Miocene (*c.* 10 Ma), the latter clade started to evolve in the most diverse *Ricotia* core clade (6 spp.), the process preceded by a DD event to $n = 13$. It is noteworthy that this dysploidy was mediated by a unique chromosomal rearrangement, merging together the same two chromosomes as were merged during the origin of a fusion chromosome within the paternal $n = 7$ genome *c.* 20 Ma. This shows that within a time period of *c.* 8 Myr genome evolution can repeat itself and that structurally very similar chromosomes may originate repeatedly from the same ancestral chromosomes by different pathways (end-to-end translocation versus nested chromosome insertion).

Keywords: karyotype evolution, hybridization, ancient polyploidy, diploidization, chromosomal rearrangements, dysploidy, *Ricotia*.

INTRODUCTION

Polyploidization, via intra- or inter-species hybridization (i.e. auto- or allopolyploidy), is one of the speciation mechanisms that is particularly common among angiosperm plants. Over short evolutionary time periods, polyploid cytotypes and species may produce higher-level polyploids, such as hexaploids, octoploids and even higher ploidies. Over longer evolutionary time periods, polyploidization or whole-genome duplication is usually followed by a genome-wide process of (re)diploidization. Diploidization is the transformation of the polyploid genome to a structurally and functionally diploid genome (e.g., Renny-Byfield *et al.*, 2013; Wendel, 2015; Soltis *et al.*, 2016; Mandáková and Lysak, 2018). Although the cyclic polyploidization–diploidization process is constantly and repeatedly concealing the polyploid nature of all seed plants, it also makes the term 'diploid' elusive and tightly bound to a given observation time point.

Post-polyploid structural diploidization is mediated by double-strand break (DSB) misrepair, acting both within and between the parental subgenomes. The resulting chromosomal rearrangements (CRs) steadily or abruptly modify the duplicated structure of a polyploid genome through deletions, duplications, inversions and translocations. In particular, chromosome translocations play the crucial role in the evolutionary fixed decrease of chromosome numbers, i.e. descending dysploidy (DD). Although chromosome translocations are thought to be a well-researched and somewhat old-fashioned topic from W.R.B. Robertson's and C.D. Darlington's times (e.g. Robertson, 1916; Darlington, 1937), we still do not understand much about where, when and why they occur. Similarly, although fixed homozygous translocations may contribute to reproductive isolation and speciation (White, 1978; Guerrero and Kirkpatrick, 2014), the causal link between translocation-mediated dysploidy and speciation is usually hard to prove. In species or genera sharing the same type of dysploid translocation event(s), however, usually it can be concluded that the shared dysploid event has pre-dated

species radiation or cladogenesis (e.g., Mandáková and Lysak, 2008; Ahola *et al.*, 2014; Stankiewicz, 2016; Mandáková *et al.*, 2017a,b).

The relationship between chromosome translocations and cladogenetic events is usually studied in well-diploidized polyploids, i.e. paleopolyploids, such as close relatives of Arabidopsis (Lysak *et al.*, 2006), Prospero (Jang *et al.*, 2013), grasses (Luo *et al.*, 2009; Betekhtin *et al.*, 2014; Winterfeld *et al.*, 2018) and other angiosperms (Murat *et al.*, 2017). The disadvantage of these models is that despite their ancient polyploid origin, the most recent steps of DD are actually only further reducing the number of chromosomes in already fully diploidized genomes. On the contrary, frequently observed karyological instability in neopolyploids, such as compensating aneuploidy and inter-subgenome CRs (e.g. Xiong *et al.*, 2011; Chester *et al.*, 2012; Mandáková *et al.*, 2014), does not provide a sufficient clue indicating which of the documented CRs will become evolutionary fixed. These limitations are less constraining in mid-aged polyploids, i.e. mesopolyploids, where the parental subgenome structure remains discernible, but at the same time continuing re-diploidization has already modified the polyploid genome landscape, usually with different intensities and rates specific to individual species or (sub)clades (e.g., Lysak *et al.*, 2007; Mandáková *et al.*, 2010a,b, 2017a,b; Mandáková and Lysak, 2018). Indeed, mesopolyploid genomes and clades may allow us to reconstruct pathways and underlying mechanisms of post-polyploid structural diploidization with more certainty than in paleo- or neopolyploid genomes.

The small mesopolyploid genus *Ricotia* (Brassicaceae, expanded lineage II, tribe Biscutelleae; Özüdoğru *et al.*, 2017), comprising nine species distributed in the eastern Mediterranean (Figure 1a), provides some new insights into the mechanism of post-polyploid genome evolution and the role of CRs in plant cladogenesis. As *Ricotia* species are rather heterogenous in terms of biological, ecological and geographic traits (Özüdoğru *et al.*, 2015, 2016), the genus provides an opportunity to test several hypotheses on post-polyploid plant genome evolution. For instance, the disjunctive distribution of the nine species, including two island endemics (*Ricotia cretica* and *Ricotia isatoides*), the infrageneric karyological variation ($2n = 26$ and 28), and perennials versus annuals associated with higher and lower altitudes, respectively, provoke the question of whether these differences are also reflected by inter-species genome differentiation.

In the present study, we aimed to focus on the following questions and aspects of genome evolution in the mesopolyploid *Ricotia*: (i) what are the genome structures of the nine species, and do they reflect infrageneric phylogenetic relationships; (ii) what structure did the ancestral *Ricotia* genome have, and how and when did it originate (e.g. auto- versus allopolyploid origin; identity of parental genomes); (iii) what were the mechanisms and rates of post-polyploid diploidization; (iv) does the ecogeographic differentiation (e.g. lowland versus high-elevation species; mainland versus island species) correlate with the interspecies genome differentiation?

To achieve these targets, we carried out comparative chromosome painting (CCP) analysis of seven *Ricotia* species representing the full phylogeographic diversity of the genus. To bolster our analyses and interpretations, plastome sequences were used to build up a maternal phylogeny of *Ricotia*, complementing previous phylogenetic studies based on one nuclear and one plastid gene (Özüdoğru *et al.*, 2015).

RESULTS

Dated plastid phylogeny

To follow the maternal origin of *Ricotia* species, we concatenated 77 plastid genes into a matrix that contained 61 020-bp gap-free sites, and conducted phylogenetic analysis using maximum likelihood (ML) and Bayesian methods. All nodes within the genus received 100% bootstrap support and a posterior probability of 1.0 in ML and Bayesian trees, respectively (Figure 1b). Within *Ricotia*, the Aucheri clade (*Ricotia aucheri*) is sister to all other species, and the Tenuifolia clade (*R. isatoides* and *Ricotia tenuifolia*) is sister to the remaining species, namely *Ricotia carnosula*, *R. cretica*, *Ricotia davisiana* and *Ricotia lunaria* (hereafter referred to as the *Ricotia* core clade). The three retrieved infrageneric clades were congruent with the phylogenetic analysis published earlier (Özüdoğru *et al.*, 2015). Within Brassicaceae, *Ricotia* is placed within the monophyletic tribe Biscutelleae, which is sister to other species of clades B, C and D (Figure S1).

Our molecular dating analysis (Figure 1b; Table 1) suggested that *Ricotia* diverged from other genera of Biscutelleae at *c.* 21.19 Ma, and the crown age of this genus is around 17.8 Ma. The Tenuifolia clade and the *Ricotia* core clade diverged at *c.* 15.88 Ma. The divergence of the Crete endemic *R. cretica* from its closest congener *R. carnosula* was dated to *c.* 4.97 Ma.

Genome structure of seven *Ricotia* species

Two different chromosome numbers were identified in *Ricotia*: $2n = 28$ in Aucheri (*R. aucheri*) and Tenuifolia clades (*R. isatoides*, *R. tenuifolia*), and $2n = 26$ in four core-clade species (*R. cretica*, *R. davisiana*, *R. lunaria* and *R. sinuata*). Several erroneous reports of $2n = 28$ were presumably reported as a result of the fragility of the large interstitial nucleolar organizer region (NOR; 35S rDNA),

(a)

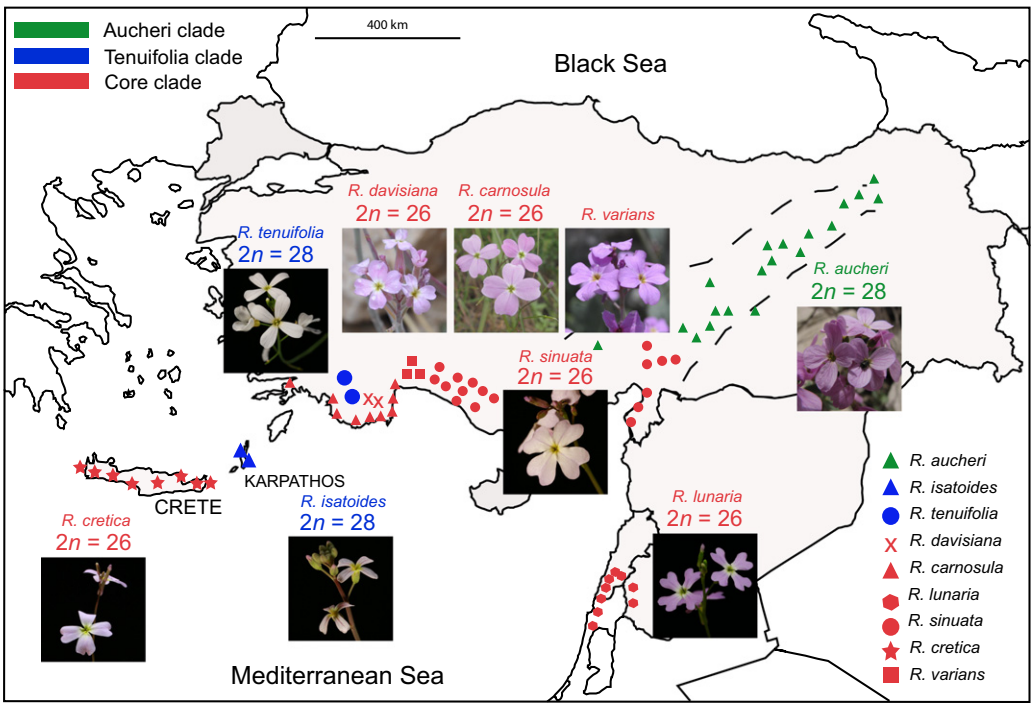

(b)

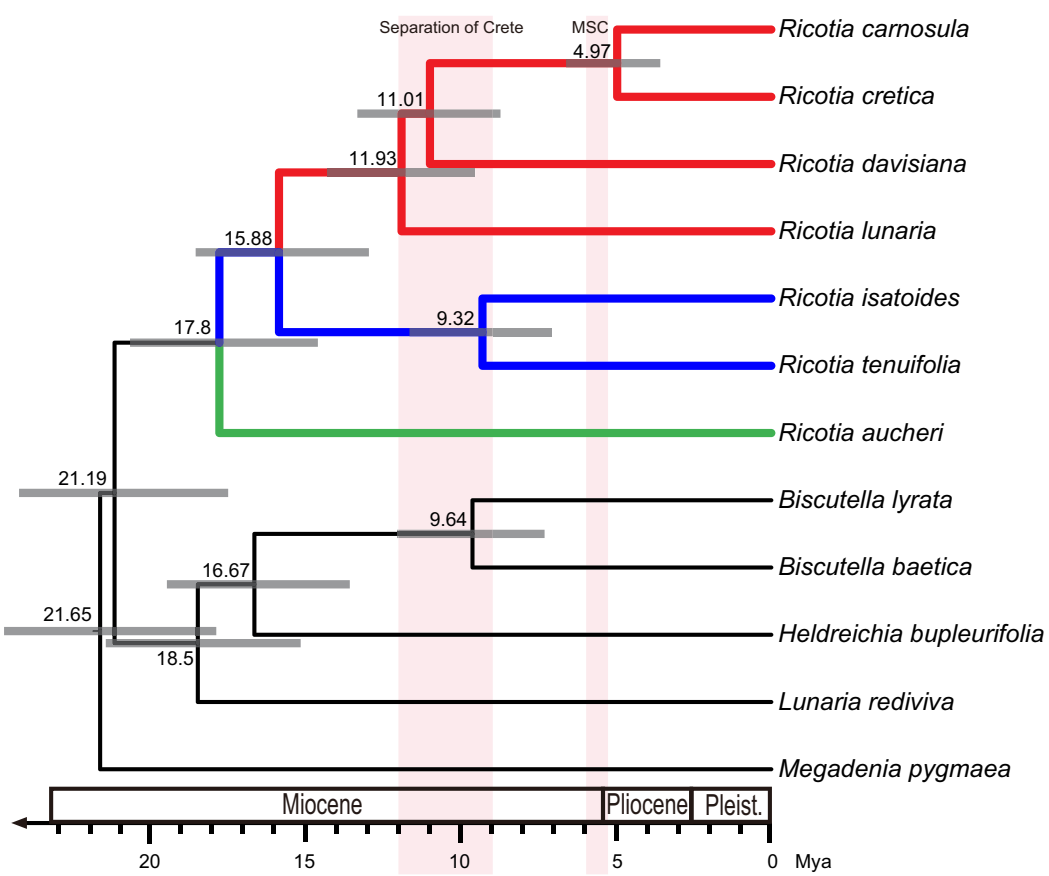

Figure 1. Distribution and phylogenetic relationships of *Ricotia* species.
(a) Distribution of three infrageneric clades and nine *Ricotia* species (adapted from Özüdoğru *et al.*, 2015).
(b) Dated plastid phylogeny of *Ricotia* and the tribe Biscutelleae. The BEAST analysis of a concatenated 77-gene matrix is shown. All nodes are supported with a posterior probability of 1.0. Divergence times (million years ago, Mya) are displayed with 95% high posterior density intervals. The time span of two geological events, i.e. the separation of Crete and the Messinian Salinity Crisis (MSC), are indicated. Branches leading to three infrageneric *Ricotia* clades are labeled with red, blue and green, respectively. Pleist., Pleistocene.

Table 1 Divergence time estimates for *Ricotia* and the tribe Biscutelleae based on the plastid phylogeny (Figure 1b). Age estimates are indicated with means (in bold) and 95% highest posterior densities (HPDs). For secondary calibration, the estimates for the origin of clade B and the family were based on data from Guo *et al.* (2017). For paleobiogeographic calibration, we used the time when the island of Crete was completely isolated from the neighbouring landmasses (*c.* 5.3 Ma) to calibrate the split between *Ricotia carnosula* and *Ricotia cretica*

	Secondary calibration	Paleobiogeographic calibration
R. cretica versus *R. carnosula*	3.58 – **4.97** – 6.62	3.86 – **4.9** – 5.57
Ricotia core clade	9.55 – **11.99** – 14.34	10.12 – **12.72** – 15.98
Tenuifolia versus core clade	12.98 – **15.88** – 18.57	13.78 – **17.09** – 21.3
crown Tenuifolia	7.14 – **9.32** – 11.72	7.51 – **9.99** – 13.02
crown *Ricotia*	14.63 – **17.8** – 20.69	15.53 – **19.2** – 23.92
crown Biscutelleae	17.9 – **21.65** – 24.75	19.06 – **23.47** – 29.2
Biscutelleae versus clade B + C + D	19.68 – **23.71** – 26.93	20.9 – **25.68** – 31.88

whereby the broken-off terminal parts of the NOR-bearing chromosome pair were mistaken for an extra chromosome pair (Figure S2a).

Comparative cytogenetic maps for seven *Ricotia* species were constructed by CCP based on fluorescence *in situ* hybridization (FISH) localization of chromosome-specific bacterial artificial chromosome (BAC) contigs of *Arabidopsis thaliana* (for examples of CCP, see Figure S3). The painting probes were designed to reflect the system of 22 ancestral genomic blocks (GBs) building up eight chromosomes of the reference Ancestral Crucifer Karyotype (ACK) genome (Schranz *et al.*, 2006; Lysak *et al.*, 2016). The constructed cytogenetic maps (Figure 2) were compared with the known ancestral karyotypes in Brassicaceae: ACK (n = 8), ancestral Proto-Calepineae Karyotype (ancPCK, n = 8; Geiser *et al.*, 2016), Proto-Calepineae Karyotype (PCK, n = 7; Mandáková and Lysak, 2008) and translocation Proto-Calepineae Karyotype (tPCK, n = 7; Cheng *et al.*, 2013).

In all *Ricotia* species analyzed, all 22 GBs were found in duplicates within their haploid chromosome complements. This points to a tetraploid origin of *Ricotia*. In all species analyzed, homeologous GBs slightly differed in physical length (Figure S3); however, the differences were subtle as compared with other mesopolyploid Brassicaceae species with a higher degree of diploidization (Mandáková *et al.*, 2010a, 2017a,b; Geiser *et al.*, 2016). This is most likely reflecting a slow rate of post-polyploid diploidization, including biased subgenome fractionation.

In *R. aucheri* (n = 14; Figure 2), eight chromosomes structurally resembled the ancestral chromosomes of ACK (two homeologs of AK1, AK2 and AK4, and one homeolog of AK3 and AK7), two chromosomes had the structure of the AK6/8 chromosome with GB association O + P + Wb + R, as in the ancPCK and PCK genomes (Mandáková and Lysak, 2008; Geiser *et al.*, 2016), and the remaining four chromosomes originated by *R. aucheri*-specific CRs among five ancestral chromosomes: AK3, AK5, AK7, AK8/6 and AK5/8/6.

Karyotypes of two species from the Tenuifolia clade (*R. isatoides* and *R. tenuifolia*, both n = 14; Figure 2) shared nine chromosomes with the ACK genome (two homeologs of AK1, AK3 and AK4, and one homeolog of AK2, AK5 and AK7), two homeologs of ancPCK and PCK-like chromosome AK6/8, one ancPCK-specific chromosome AK8/6 (with GB association V + Wa + Q + X; Geiser *et al.*, 2016), and one PCK-specific chromosome AK5/8/6 (with GB association M – N + V + K – L + Wa + Q + X; Mandáková and Lysak, 2008). One Tenuifolia-specific chromosome (AK2/7) was formed by a nested chromosome insertion (NCI) involving 'insertion' AK2 and 'recipient' AK7 chromosomes, respectively. The NCI event, mediated by two breaks within the subtelomeric regions of AK2 and one in the AK7 (peri)centromere, was later followed by a pericentric inversion. We note that no heterochromatic knobs, unpainted regions or interstitial telomeric repeats were identified at the translocation breakpoints on both arms of AK2/7.

In four analyzed *Ricotia* core-clade species (*R. cretica*, *R. davisiana*, *R. lunaria* and *R. sinuata*, all n = 13; Figure 2), the karyotypes resembled Tenuifolia genomes, except for the reduced number of chromosomes to 13. This DD was mediated by an NCI event involving chromosomes AK5 and ancPCK-specific AK8/6, later followed by a para- and pericentric inversion, respectively. Interestingly, one breakpoint (originally in the subtelomeric region of the bottom

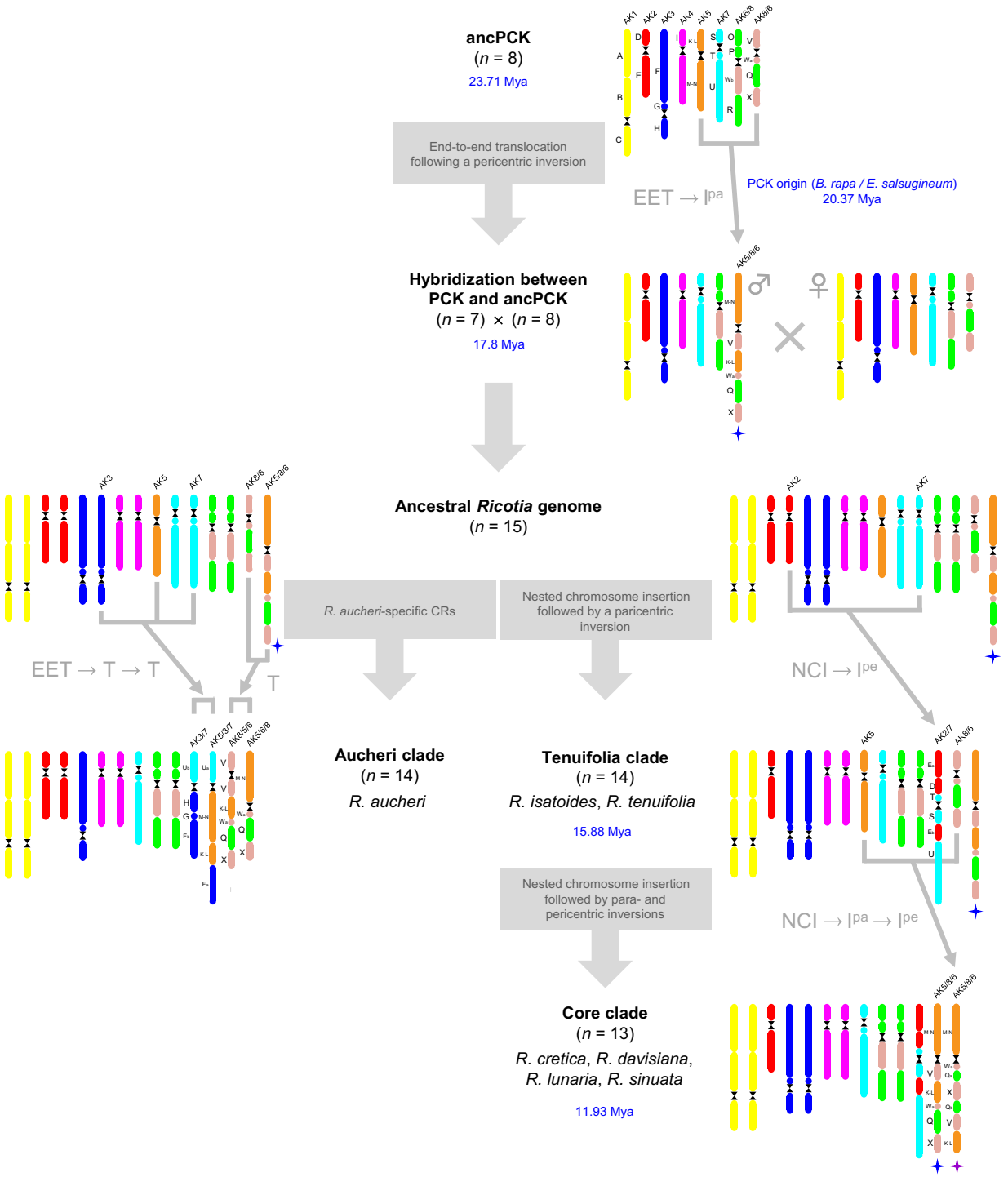

Figure 2. Reconstructed origin of the *Ricotia* ancestral genome and its subsequent evolution.
The color code and capital letters correspond to the eight chromosomes and 22 genomic blocks of the Ancestral Crucifer Karyotype (ACK), respectively (Lysak *et al.*, 2016). The PCK- and *Ricotia*-specific chromosome AK5/8/6 is indicated by a blue and violet four-point star, respectively. The divergence time estimates are taken from Tables 1 and S1. Abbreviations: I^{pa}, paracentric inversion; I^{pe}, pericentric inversion; Mya, million years ago; NCI, nested chromosome insertion; T, chromosome translocation.

arm of AK8/6) was reused in each of the three steps towards the origin of fusion chromosome AK5/8/6 (blue arrows in Figure 3a).

All seven *Ricotia* species uniformly bear a large interstitial locus of 35S rDNA on AK7 homeolog and between two and eight 5S rDNA interstitial loci on different

chromosomes (Figure S2b). The evolutionarily conserved position of NORs indicates that 35S rDNA repeats were not involved in the clade-specific CRs described above.

Ancestral *Ricotia* genome and its allopolyploid origin

The presence of both ancPCK- and PCK-specific CRs in all *Ricotia* genomes analyzed strongly suggests an allopolyploid origin of the genus. The most recent common ancestor (MRCA) of modern *Ricotia* species originated via hybridization between the ancPCK ($n = 8$) and PCK ($n = 7$) genomes (Figures 2 and 4). As the modern genomes of *Biscutella* (Geiser *et al.*, 2016) and two other Biscutelleae genera (*Heldreichia* and *Lunaria*) are descendants of ancestral polyploid genomes based exclusively on the ancPCK genome, and the maternal phylogeny supported the monophyly of the Biscutelleae (Figures 1b and S1; Özüdoğru *et al.*, 2017), ancPCK ($n = 8$) was most likely the maternal parent of the ancestral *Ricotia* allotetraploid.

By comparing the karyotype structures of the species analyzed, we inferred a putative genome structure of the *Ricotia* MRCA. As the Tenuifolia clade exhibits the highest number of non-reshuffled ancestral chromosomes among the three *Ricotia* clades (Figure 2), the genome of the MRCA must have been structurally closest to Tenuifolia karyotypes; however, the AK2/7 chromosome – clearly a fusion chromosome – is pointing to the existence of 15 chromosome pairs in the ancestral *Ricotia* genome. This is further supported by AK2 and AK7 still being retained as individual chromosomes in *R. aucheri* (Figure 2), the most ancestral *Ricotia* clade (Figure 1b).

Independent origin of PCK-like chromosome AK5/8/6 in the *Ricotia* core clade

The ancestral *Ricotia* genome as well as genomes of the extant species contain chromosome AK5/8/6 (GB association M – N + V + K – L + Wa + Q + X), contributed by the paternal PCK subgenome. The PCK-specific chromosome originated from AK5 and AK8/6 chromosomes of the ancPCK genome ($n = 8$), either by Robertsonian-like translocation preceded by a pericentric inversion (Mandáková and Lysak, 2008) or, more likely, by end-to-end translocation (EET) between short arms of AK5 and AK8/6, followed by the inactivation of the AK8/6 centromere. Breakpoints of the subsequent paracentric inversion occurred at the site of the inactive AK8/6 paleocentromere (between GBs V and Wa) and (peri)centromere of the fusion chromosome (Figures 2 and 3a).

Interestingly, during the evolution of the *Ricotia* core-clade genome from the older Tenuifolia genome, a fusion chromosome structurally resembling the PCK-specific chromosome AK5/8/6 was formed from the identical AK5 and AK8/6 chromosomes within the ancPCK maternal subgenome (Figures 2 and 3a–c). The chromosome originated via an NCI, involving the 'insertion' chromosome AK8/6 and the 'recipient' chromosome AK5. The NCI was mediated by a break at the AK5 (peri)centromere and two breaks at subtelomeric regions of AK8/6, followed by a peri- and paracentric inversion, respectively (Figure 3a–c).

Although the mechanisms (EET versus NCI) as well as the inversion breakpoints underlying the origin of both fusion chromosomes differed, the top and bottom arms of both chromosomes are composed of the identical GBs. The initial step in the origin of both fusion chromosomes involved a shared breakpoint within the subtelomeric region of the short arm of the ancPCK-specific chromosome AK8/6 (red arrows in Figure 3a).

Each of the two fusion events was associated with the inactivation of different paleocentromeres. The origin of PCK-specific chromosome AK5/8/6 by EET was associated with the inactivation of the AK8/6 paleocentromere, whereas the *Ricotia*-specific chromosome AK5/8/6 originated by NCI disrupting the AK5 paleocentromere. The inactivation/removal of both paleocentromeres left no remnants in the form of heterochromatic arrays or interstitial telomeric repeats (Figure 3b; Mandáková and Lysak, 2008).

DISCUSSION

Origin of the ancestral *Ricotia* genome via an inter-clade hybridization

All the extant *Ricotia* species as well as the reconstructed ancestral genome of *Ricotia* consist of 22 duplicated GBs. This unequivocally points to the origin of the whole genus from a tetraploid ancestor. As the 15-chromosome genome of the MRCA of *Ricotia* combines chromosomes specific for two ancestral genomes, ancPCK ($n = 8$; Geiser *et al.*, 2016) and PCK ($n = 7$; Mandáková and Lysak, 2008), we propose that *Ricotia* originated by hybridization between members of ancPCK ($n = 8$) and PCK ($n = 7$) clades (Figure 4). As the PCK genome itself evolved from the more ancient ancPCK genome, this inter-clade hybridization can be vaguely classified as backcrossing with a time lag (*c.* 2.6 million years). Whereas the ancPCK genome was identified as an ancestral genome of *Biscutella* (Geiser *et al.*, 2016), *Ricotia* (this study) and most likely the other three Biscutelleae genera, the PCK genome is specific for the bona fide monophyletic (expanded) lineage II/clade B (Mandáková and Lysak, 2008). Historically, the co-occurrence and hybridization between ancPCK- and PCK-like genomes is fully compatible with the past as well as extant presence of four (*Biscutella*, *Heldreichia*, *Lunaria* and *Ricotia*) of the five Biscutelleae genera (Özüdoğru *et al.*, 2017) in the Western Irano-Turanian region and eastern Mediterranean, together with numerous (expanded) lineage-II tribes. In addition, the Irano-Turanian region was the most probable cradle and evolutionary melting pot of the

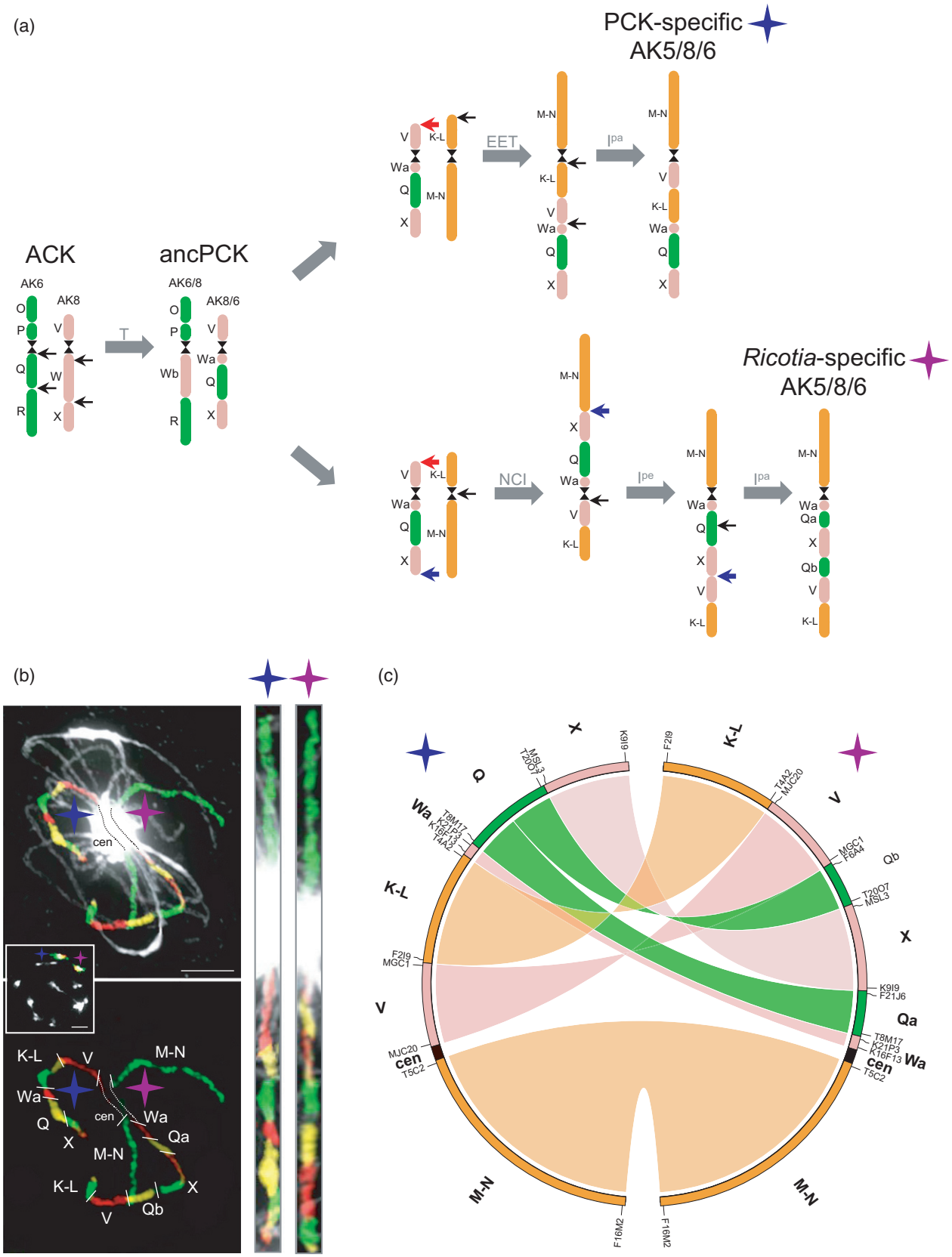

Figure 3. The independent origin of fusion chromosome AK5/8/6 during the evolution of the PCK (n = 7) and core-clade *Ricotia* genomes (n = 13).
(a) Parsimoniously reconstructed origins of PCK- and *Ricotia*-specific chromosome AK5/8/6. Reused breakpoints of the inferred chromosomal rearrangements (CRs) are shown by red (shared between the two AK5/8/6 chromosomes) and blue (reused during the formation of the *Ricotia*-specific AK5/8/6) arrows. Abbreviations: EET, end-to-end translocation; I^{pa}, paracentric inversion; I^{pe}, pericentric inversion; NCI, nested chromosome insertion.
(b) Comparative chromosome painting identifying PCK- and *Ricotia*-specific chromosome AK5/8/6 in *Ricotia cretica* (2n = 26). Each chromosome is visible as a synapsed bivalent at pachytene or diakinesis (inset). Red, green and yellow colors correspond to epifluorescences of biotin-, digoxigenin- and Cy3-labeled painting bacterial artificial chromosome (BAC) contigs. Chromosomes were counterstained by 4′,6-diamidino-2-phenylindole (DAPI). Scale bar: 10 μm.
(c) Circos plot displying the collinearity between PCK- and *Ricotia*-specific fusion chromosomes AK5/8/6. The individual genomic blocks are specified by *Arabidopsis thaliana* BAC clones. The color code – only in (a) and (c) – and capital letters correspond to the eight chromosomes and 22 genomic blocks of the Ancestral Crucifer Karyotype (ACK), respectively (Lysak *et al.*, 2016). cen, centromere.

Brassicaceae family (Franzke *et al.*, 2009; Mohammadin *et al.*, 2017). Narrowing down the ancestral range of *Ricotia* (see Figure 1a), two scenarios materialize based on previous (Özüdoğru *et al.*, 2015) and present studies: (i) the *Ricotia* allotetraploid originated in the Anatolian Diagonal mountains, with *R. aucheri* representing a living remnant in this region; or (ii) the *Ricotia* species diversity centre in southern Turkey roughly overlaps with the ancestral species ranges, and *R. aucheri* migrated north-east towards its present-day area. As exemplified by the long-distant migration of *R. lunaria* to its current distribution in Lebanon and Israel, *Ricotia* species may have dynamically changed their distribution ranges in the past. The origin and evolution of *Ricotia* genomes are compatible with both paleobiogeographic scenarios: the genus originated either on the Anatolian Plateau or in the adjacent Aegean/Mediterranean region (Özüdoğru *et al.*, 2015).

Although not frequent in the Brassicaceae, at least two other ancient inter-clade or inter-tribal hybridizations were documented in the family, namely the allopolyploid origin of the tribes Shehbazieae (German and Friesen, 2014) and Microlepidieae (Mandáková *et al.*, 2017b). In the latter event, hybridization between n = 8 and n = 7 genomes and the origin of an ancestral allotetraploid n = 15 genome closely resemble the origin of *Ricotia*.

A repeated fusion of the same ancestral chromosomes after 8 million years

The genomes of *Ricotia* core-clade species are noteworthy by the presence of two seemingly very similar chromosome pairs, both named AK5/8/6. Our analyses, however, uncovered that the origin of the two chromosomes must have been independent and separated by roughly 8 million years. Whereas one fusion chromosome pair was inherited from the paternal PCK-like genome, formed before the divergence of lineage II (*c.* 20.37 Ma; Table S1), the second chromosome originated within the Tenuifolia-clade genome, prior to the diversification of the core clade *c.* 12 Ma (Figure 4). In both genomes, the fusion AK5/8/6 chromosomes originated by a merger of chromosomes AK5 and AK8/6 within the ancPCK (sub)genome, mediated by different translocation mechanisms and further reshuffled by different inversions.

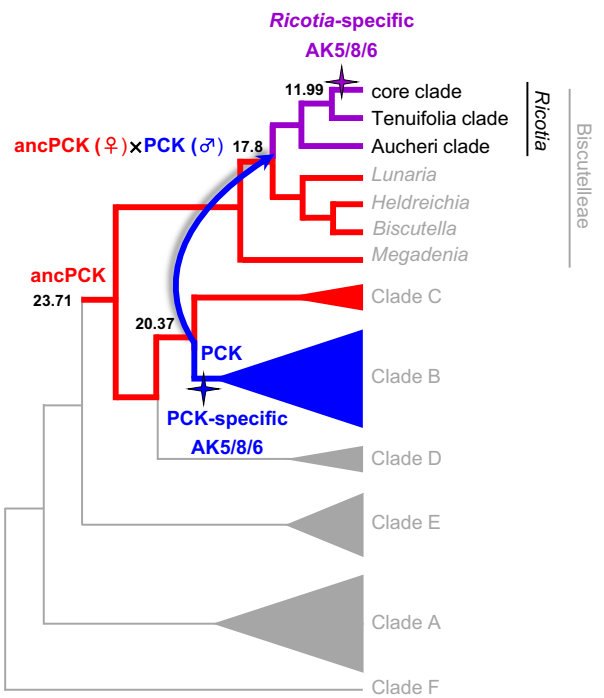

Figure 4. The allopolyploid origin of *Ricotia* and repeated formation of fusion chromosome AK5/8/6 in the phylogenetic context of the entire family.
The PCK- and *Ricotia*-specific chromosome AK5/8/6 is indicated by a blue and violet four-point star, respectively. The phylogenetic scheme is based on the dated maternal phylogeny (Figures 1B and S1; Tables 1 and S1). Numbers refer to million years ago.

This observation shows that structurally identical or similar fusion chromosomes may be formed in land plants from the same precursor chromosomes by different translocation mechanisms repeatedly after several million years. Moreover, our data demonstrate that a recurrent chromosome fusion can take place in a diploid ancestral genome as well as within the same (sub)genome several million years after a polyploidization event. The recurrence of the reciprocal translocation between chromosome arms 4L and 5L, accompanied by the reuse of breakpoints, was reported for Triticeae species (Li *et al.*, 2016). Although these were much simpler CRs than the independent

formation of AK5/8/6 chromosomes, both instances suggest that some recurrent CRs can be selected for repeatedly.

Descending dysploidy via nested chromosome insertion in *Ricotia* and other Brassicaceae taxa

Recurring NCIs were common during grass genome evolution as the prevailing mechanism of DD (Luo *et al.*, 2009; International Brachypodium Initiative 2010; Betekhtin *et al.*, 2014), but have been only rarely reported in other angiosperm families (Cucurbitaceae: Yang *et al.*, 2014; Fabaceae: Fonsêca *et al.*, 2016). In Brassicaceae, few NCI events were described, e.g. in *Hornungia alpina* (chromosome AK2/5; Lysak *et al.*, 2006), *Pachycladon* (AK2/3; Mandáková *et al.*, 2010b) or *Cardamine pratensis* (AK5/8/5; Mandáková *et al.*, 2013). An NCI event requires at least three DSBs – two at subtelomeres of an 'insertion' chromosome and one at the (peri)centromere of the 'recipient' chromosome – and specific conditions ensuring that the two chromosome ends recombine with sequences at the 'recipient' pericentromere. In *Ricotia*, two DDs leading to a $n = 14$ and $n = 13$ genome in the Tenuifolia and core-clade species, respectively, were mediated by NCI. As both events involved two different pairs of ancestral chromosomes, we can only hypothesize that the occurrence of NCIs in *Ricotia* and other angiosperm species is pre-determined by the spatial arrangement of interphase or meiotic chromosomes, rather than by the propensities of the chromosomes.

A slow rate of structural diploidization in *Ricotia*

Based on our dated phylogeny (Figure 1b), the ancestral allotetraploid genome of *Ricotia* was formed around 17.8 Ma, whereas the youngest species split (*R. carnosula*–*R. cretica*) occurred at just 4.97 Ma. This is a time span of more than 10 million years. The first two independent DDs (from $n = 15$ to $n = 14$), marking the divergence of the Aucheri and Tenuifolia clades, occurred within 2 million years after the origin of the allotetraploid genome. More rearrangements in *R. aucheri* compared with the Tenuifolia clade species suggest an accelerated tempo of post-polyploid diploidization in the Aucheri clade and genome stasis in the Tenuifolia clade. The core-clade-specific DD (from $n = 14$ to $n = 13$) occurred approximately 4 million years after the preceding Tenuifolia-specific dysploidy, and all core-clade genomes remained structurally stable until present.

Comparison of *Ricotia* and *Biscutella* genomes (Geiser *et al.*, 2016) offers some parallels, but at the same time tells different stories. Both Biscutelleae genera have evolved from different tetraploid progenitor genomes, with $n = 15$ (*Ricotia*) and $n = 16$ (*Biscutella*). Whereas the allotetraploid ancestor of *Ricotia* originated by hybridization between ancPCK and PCK genomes, the *Biscutella* tetraploid was most likely formed by auto- or allopolyploidization involving two ancPCK(-like) genomes (Geiser *et al.*, 2016). The origin of the *Ricotia* tetraploid ancestor was dated to the Early to Middle Miocene (*c.* 17.8 Ma), whereas the tetraploid ancestor of *Biscutella* originated during the Late Miocene (*c.* 8 Ma; Geiser *et al.*, 2016). Both independent polyploidization events were followed by two species radiations: a larger one in *Biscutella* (with approximately 45 extant species, mostly occurring in the western Mediterranean) and a smaller one in *Ricotia* (with only nine extant species, occurring in the eastern Mediterranean). The level of DD in *Biscutella*, ranging from 1.7- to 2.6-fold (i.e. from $n = 16$ to $n = 9$, 8 and 6), is much more extensive than in *Ricotia* (ranging from 1.07- to 1.15-fold, i.e. from $n = 15$ to $n = 14$ and 13), and hence must have proceeded much faster in *Biscutella* than in *Ricotia*. We hypothesize that homeologous recombination between two identical or very similar ancPCK-like subgenomes in *Biscutella* have been more frequent than recombination between two well-differentiated parental subgenomes in *Ricotia*. However, in the Southern Hemisphere analogue of *Ricotia* – the tribe Microlepidieae – even the least diploidized mesotetraploid genome of the perennial *Arabidella* species represents a 1.25-fold reduction (from $n = 15$ to $n = 12$), however. Considering the younger Late Miocene age of the Microlepidieae (i.e. 10.6–7.52 Ma), we have to conclude that the rate of post-polyploid diploidization in *Ricotia* was slower than the slowest diploidization in the Microlepidieae. All such comparisons however do not reflect various inexplicable extrinsic (and intrinsic) factors which may trigger and/or accelerate the diploidization process.

Descending dysploidies presumably triggered cladogenesis in *Ricotia* but were less important for speciation

The position of the three dysploid events at the base of three infra-generic clades identifies the reductions of chromosome number as potentially important drivers of cladogenesis in *Ricotia*. Indeed, the reduced number of chromosomes has multiple effects, such as altered recombination frequencies, new gene linkage or modified gene expression regulation on newly formed fusion chromosomes (e.g. Guerrero and Kirkpatrick, 2014; Mandáková *et al.*, 2017b). On the contrary, as all four core-clade species analyzed, including species geographically as distant as *R. cretica* (Crete) and *R. lunaria* (Lebanon/Israel), share the same genome structure, we conclude that the six speciation events in this clade were not associated with major CRs. Similarly, the divergence between *R. isatoides* and *R. tenuifolia* was not associated with major CRs. This suggests that despite the apparent geographic and environmental gradients across the distribution range for *Ricotia*, partly diploidized *Ricotia* genomes remain structurally unchanged for 16 (Tenuifolia clade) to 12 (the core clade) million years.

Multiple paleobiogeographic scenarios provide only limited insights into genome evolution in the island *Ricotia* species

The fact that two of the nine *Ricotia* species are island endemics allowed us to explore whether the insular isolation can provide an additional insight into the rate of karyotype evolution in these species. The major cladogenetic and speciation events in *Ricotia* were dated to commence during the Early Miocene, and the most recent species split (4.97 Ma) occurred in the Pliocene. In the Early to Middle Miocene, Asia Minor and the present-day Aegean Islands, Crete and the Peloponnese represented a continuous stretch of land, the Ägäis (e.g. Cellinese *et al.*, 2009; Crowl *et al.*, 2015; Sfenthourakis and Triantis, 2017), and this landmass existed at the time of the purported origin of *Ricotia*, dated between 20.7 and 14.6 Ma. Approximately 12 Ma, as the waters of the Mediterranean innundated Ägäis, today's Crete was separated from Karpathos' island complex, and by 8 Ma the Cretan group of islands was isolated by the sea (Kougioumoutzis *et al.*, 2018; Sfenthourakis and Triantis, 2017). During the Messinian Salinity Crisis (MSC; 5.93–5.33 Ma), when the whole Mediterranean basin desiccated, the Aegean Islands and Asia Minor were connected by numerous land bridges, facilitating dispersal events; however, Crete was surrounded by saline deserts or saline/hypersaline lakes during the MSC (Kougioumoutzis *et al.*, 2018), hampering dispersal events from and to Crete. A rapid re-flooding at 5.33 Ma restored the isolation of many islands, including Crete.

In the bispecific Tenuifolia clade, *R. tenuifolia* is restricted to the Turkish mainland, whereas *R. isatoides* is endemic to Karpathos. The origin of the two species, sharing the same $n = 14$ genome, was dated to occur *c.* 9.32 Ma, which is when Karpathos and Rhodos were still connected to the Anatolian mainland. Karpathos has become completely isolated from Rhodos during the late Pliocene (3.6–2.58 Ma; Beerli *et al.*, 1996; Kougioumoutzis *et al.*, 2018). The most plausible scenario includes the divergence of both *Ricotia* species on the Anatolian mainland, the migration of *R. isatoides* to present-day Karpathos and the extinction of the mainland populations. This scenario would suggest that *R. isatoides* remained isolated on Karpathos for about the last 3 million years, with no major CRs differentiating both sister species.

Ricotia cretica, endemic to Crete, shares the $n = 13$ genome with three other core-clade species analyzed, and was retrieved as a sister species of *R. carnosula*. The core-clade genome originated *c.* 12 Ma (14.34–9.55 Ma) on the Turkish mainland, in the time when Crete was still connected with the mainland and migration of an ancestral species to Crete was feasible. It can be assumed that an ancestral core-clade species spread from the mainland to present-day Crete prior to or during the MSC, and that the isolation of Crete at the end of the MSC (5.33 Ma) triggered the *R. carnosula*/*R. cretica* divergence at 4.97 Ma (6.62–3.58 Ma). Thus, *R. cretica* remained isolated on Crete at least for the last 5.33 million years without major alterations of its genome, as compared with *R. carnosula* and other core-clade species.

In summary, genome stasis among island and mainland species as well as multiple opportunities of dispersals from the Anatolian mainland to Crete and Karpathos provides only a limited insight into the role of insular isolation on genome evolution in *Ricotia*.

EXPERIMENTAL PROCEDURES

Plastome assembly and annotation

Leaf material of seven *Ricotia* species (Table S2) was harvested and dried using silica gel. Total DNA was extracted using a Qiagen DNA isolation kit (Qiagen, https://www.qiagen.com). Sequencing was performed on the Illumina HiSeq2000 sequencer by Admera Health (https://www.admerahealth.com). Short paired-end reads (2×150 bp) were generated for each sample by low-coverage whole-genome sequencing (*c.* $0.1 \times$). Low-quality reads and potential adapters were filtered using TRIMMOMATIC 0.32 (Bolger *et al.*, 2014), with default parameters. The clean reads were assembled into complete plastome by NOVOPLASTY 1.1 (Dierckxsens *et al.*, 2016) using default parameters, with the plastid psbA sequence of *Megadenia pygmaea* (Guo *et al.*, 2017) as a seed. As the NOVOPLASTY software did not yield a circularized assembly for *R. cretica*, we first used VELVET 1.2.1 (Zerbino and Birney, 2008) to assemble reads into contigs with a wide range of kmers (from 79 to 145, with a step size of 11), and then merged these contigs by aligning them to the chloroplast genome of *M. pygmaea* in GENEIOUS 8.0.5 (Kearse *et al.*, 2012). The annotation was performed with PLANN 1.1.1 (Huang and Cronk, 2015) using the annotation of the *M. pygmaea* plastome as a reference, aided by manual refinement in SEQUIN (Clark *et al.*, 2016). The Aragorn web interface (Laslett and Canback, 2004) was used to predict tRNAs. The annotated plastomes of seven *Ricotia* species as well as those of *Biscutella baetica*, *Biscutella lyrata*, *Heldreichia bupleurifolia* and *Lunaria rediviva* were deposited in GenBank (accession numbers MH359178–MH359188).

Phylogenetic analysis and dating

For phylogenetic analysis we used the 77-gene matrix as previously described by Guo *et al.* (2017). We used customized PERL scripts to extract these protein-coding genes (PCGs) from GenBank formatted sequences and annotations. Besides the seven *Ricotia* plastomes assembled in this study, we also included sequences of 11 other species available from GenBank to cover all major clades of Brassicaceae (Huang *et al.*, 2016). After removing start and end codons, each PCG was aligned using PRANK 130410 (Löytynoja and Goldman, 2008), according to the translated amino acid sequences. Ambiguous alignment regions were trimmed by using GBLOCKS 0.91b (Castresana, 2000) with the (–t = c) option to set the sequence type to codons, default settings were used for everything else. Sequence alignments have been deposited to the Figshare online digital repository (https://doi.org/10.6084/m9.figshare.6270029). We used the greedy search mode implemented in PARTITIONFINDER 1.1.1 (Lanfear *et al.*, 2012) to find the best-fitting scheme of partition subsets and models to accommodate different genes and codons.

The optimal scheme as well as the concatenated 77-gene matrix were subjected to RAXML 8.2.11 (Stamatakis, 2014) to perform ML phylogenetic analysis with 1000 fast bootstrap replicates (–f a) under the general time reversible plus gamma (GTR + G) model. We used BEAST 2.4.8 (Bouckaert *et al.*, 2014) to conduct Bayesian Markov chain Monte Carlo (MCMC) analyses with parameter settings according to Hohmann *et al.* (2015).

Divergence time estimation was conducted in MCMCTREE implemented within the PAML 4.9a package (Yang, 2007) using the independent clock model (Rannala and Yang, 2007), which followed a log-normal distribution with a gamma-Dirichlet prior (Reis *et al.*, 2014) for the overall substitution rate (rgene gamma) setting at G (4, 90, 1). The three parameters (birth rate λ, death rate μ and sampling fraction ρ) in the birth–death process with species sampling were specified as 1, 1 and 0, respectively. After a burn-in period of 2 000 000 cycles, the MCMC run was sampled every 800 cycles until a total of 10 000 samples were collected. With the lack of fossil records from *Ricotia*, and even for the whole Brassicaceae, we employed a secondary calibration strategy for molecular dating. We extracted two calibration points from Guo *et al.* (2017): the crown age of Brassicaceae was set to 42.5–29 Ma, and the crown age of clade B was set to 24.5–17.2 Ma. To further assess whether (paleo)biogeographical events can be used for divergence time estimation, we set the maximum age for *R. cretica*/*R. carnosula* to ~5.3 Ma (at the end of the MSC, 5.93–5.33 Ma). For computational feasibility in both BEAST 2 and MCMCTREE analyses, we used the codon-partitioned strategy as it is favored over the gene-partitioned strategy for Brassicaceae species (Guo *et al.*, 2017). Two separate MCMC runs were compared for convergence with two different random seeds, and similar results were observed.

Chromosome preparations

Young inflorescences of *Ricotia* species (Table S2) were harvested in the field or from plants grown from seeds (*R. lunaria*) and fixed in freshly prepared ethanol : acetic acid (3 : 1) fixative for 24 h at room temperature (*c.* 18–30°C) or 4°C. Fixative was replaced by 70% ethanol and the material stored at −20°C until further use. Selected flower buds were rinsed in distilled water (twice for 5 min) and citrate buffer (10 mM sodium citrate, pH 4.8; twice for 5 min), and digested in 0.3% cellulase, cytohelicase and pectolyase in citrate buffer at 37°C for 5 h. After digestion, individual anthers were dissected on a microscope slide in 20 µl of 50% acetic acid and spread on the slide placed on a metal hot plate (50°C) for *c.* 30 s. Then, the preparation was fixed in freshly prepared ethanol : acetic acid (3 : 1) fixative by dropping the fixative around and into the drop containing the dissected material. The preparation was dried using a hair dryer and staged using a phase-contrast microscope for the presence of meiotic (pachytene, diakinesis) and mitotic chromosome spreads. Suitable slides were post-fixed in 4% formaldehyde in distilled water for 10 min and air-dried.

DNA probes

For CCP in *Ricotia*, in total 674 chromosome-specific BAC clones of *A. thaliana* were used as DNA probes. BACs were grouped into contigs according to 22 GBs of the ACK (Lysak *et al.*, 2016), but hapten- or fluorochrome-labelled individually (see below). To determine and characterize CRs and the orientation of GBs on *Ricotia* chromosomes, after initial CCP experiments, some BAC contigs were split into smaller subcontigs. The *A. thaliana* BAC clone T15P10 (AF167571) containing 35S rRNA genes was used for the *in situ* localization of NORs, and *A. thaliana* clone pCT4.2 (M65137), corresponding to a 500-bp 5S rRNA repeat, was used for the localization of 5S rDNA loci. All DNA probes were individually labelled with biotin-dUTP, digoxigenin-dUTP or Cy3-dUTP by nick translation, as described by Mandáková and Lysak (2016).

Comparative chromosome painting

Chromosome preparations were treated with 100 µg ml^{-1} RNase (AppliChem, https://www.applichemus.com) in 2 × sodium saline citrate (SSC; 20 × SSC: 3 M sodium chloride, 300 mM trisodium citrate, pH 7.0) for 60 min and with 0.1 mg ml^{-1} pepsin (Sigma-Aldrich, https://www.sigmaaldrich.com) in 0.01 M HCl at 37°C for 5 min, and then post-fixed in 4% formaldehyde in 2 × SSC for 10 min, washed in 2 × SSC twice for 5 min and dehydrated in an ethanol series (70, 90 and 100%, 2 min each). Selected labeled BAC clones were pooled and ethanol-precipitated. The pellet was resuspended in 20 µl of hybridization mix (50% formamide and 10% dextran sulfate in 2 × SSC) per slide. The probe and chromosomes were denatured together on a metal hot plate at 80°C for 2 min, and incubated in a moist chamber at 37°C overnight. Post-hybridization washing was performed in 20% formamide in 2 × SSC at 42°C. The amplification and detection of fluorescent signals followed the protocol of Mandáková and Lysak (2016). Chromosomes were counterstained with 4′,6-diamidino-2-phenylindole (2 µg ml^{-1}) in Vectashield antifade (Vector Laboratories, https://vectorlabs.com) and photographed using a Zeiss Axioimager Z2 epifluorescence microscope (Zeiss, https://www.zeiss.com) and a CoolCube camera (MetaSystems, https://metasystems-international.com). Images were acquired separately for all four fluorochromes using appropriate excitation and emission filters (AHF Analysentechnik, https://www.ahf.de). The four monochromatic images were pseudocolored and merged using Adobe PHOTOSHOP CS6 software (Adobe, https://www.adobe.com). The pachytene chromosomes in Figure 4 were straightened using the 'straighten-curved-objects' plugin in IMAGEJ (https://imagej.nih.gov/ij/) (Kocsis *et al.*, 1991).

ACKNOWLEDGEMENTS

This work was supported by a research grant from the Czech Science Foundation (grant no. P501/12/G090) and the CEITEC 2020 project (grant no. LQ1601). Computational resources were provided by CESNET LM2015042 and CERIT Scientific Cloud LM2015085, under the programme 'Projects of Large Research, Development, and Innovations Infrastructures'. We are grateful to Prof. Eviatar Nevo for providing seeds of *R. lunaria*. We thank Andreas Franzke, Petra Hloušková and Kurtuluş Özgişi for their help.

CONFLICT OF INTEREST

The authors declare no conflicts of interest.

SUPPORTING INFORMATION

Additional Supporting Information may be found in the online version of this article.

Figure S1. The chronogram (maternal phylogeny) of Brassicaceae based on 77 plastid protein-coding genes.

Figure S2. (a) Chromosome count and *in situ* localization of 35S rDNA in *Ricotia lunaria* ($2n = 26$). (b) Chromosome counts and *in situ* localization of 35S and 5S rRNA genes in seven *Ricotia* species.

Figure S3. Examples of reconstructed chromosomal structures by comparative chromosome painting applied to pachytene chromosomes in four *Ricotia* species.

Table S1. Published divergence time estimates for crucifer lineage II and expanded lineage II.

Table S2. The origin of *Ricotia* species analyzed.

REFERENCES

Ahola, V., Lehtonen, R., Somervuo, P. *et al.* (2014) The Glanville fritillary genome retains an ancient karyotype and reveals selective chromosomal fusions in Lepidoptera. *Nat. Commun.* **5**, 4737.

Beerli, P., Hotz, H. and Uzzell, T. (1996) Geologically dated sea barriers calibrate a protein clock for Aegean water frogs. *Evolution*, **50**, 1676–1687.

Betekhtin, A., Jenkins, G. and Hasterok, R. (2014) Reconstructing the evolution of *Brachypodium* genomes using comparative chromosome painting. *PLoS ONE*, **9**, e115108.

Bolger, A.M., Lohse, M. and Usadel, B. (2014) Trimmomatic: a flexible trimmer for Illumina sequence data. *Bioinformatics*, **30**, 2114–2120.

Bouckaert, R., Heled, J., Kühnert, D., Vaughan, T., Wu, C.H., Xie, D., Suchard, M.A., Rambaut, A. and Drummond, A.J. (2014) BEAST 2: a software platform for Bayesian evolutionary analysis. *PLoS Comp. Biol.* **10**, e1003537.

Castresana, J. (2000) Selection of conserved blocks from multiple alignments for their use in phylogenetic analysis. *Mol. Biol. Evol.* **17**, 540–552.

Cellinese, N., Smith, S.A., Edwards, E.J., Kim, S.T., Haberle, R.C., Avramakis, M. and Donoghue, M.J. (2009) Historical biogeography of the endemic Campanulaceae of Crete. *J. Biogeogr.* **36**, 1253–1269.

Cheng, F., Mandáková, T., Wu, J., Xie, Q., Lysak, M.A. and Wang, X. (2013) Deciphering the diploid ancestral genome of the mesohexaploid *Brassica rapa*. *Plant Cell*, **25**, 1541–1554.

Chester, M., Gallagher, J.P., Symonds, V.V., Cruz da Silva, A.V., Mavrodiev, E.V., Leitch, A.R., Soltis, P.S. and Soltis, D.E. (2012) Extensive chromosomal variation in a recently formed natural allopolyploid species, *Tragopogon miscellus* (Asteraceae). *Proc. Natl Acad. Sci. USA*, **109**, 1176–1181.

Clark, K., Karsch-Mizrachi, I., Lipman, D.J., Ostell, J. and Sayers, E.W. (2016) GenBank. *Nucleic Acid Res.* **44**, D67.

Crowl, A.A., Visger, C.J., Mansion, G., Hand, R., Wu, H.H., Kamari, G., Phitos, D. and Cellinese, N. (2015) Evolution and biogeography of the endemic *Roucela* complex (Campanulaceae: *Campanula*) in the Eastern Mediterranean. *Ecol. Evol.* **5**, 5329–5343.

Darlington, C.D. (1937) *Recent Advances in Cytology*. London: Churchill.

Dierckxsens, N., Mardulyn, P. and Smits, G. (2016) NOVOPlasty: de novo assembly of organelle genomes from whole genome data. *Nucleic Acid Res.* **45**, e18.

Fonsêca, A., Ferraz, M.E. and Pedrosa-Harand, A. (2016) Speeding up chromosome evolution in *Phaseolus*: multiple rearrangements associated with a one-step descending dysploidy. *Chromosoma*, **125**, 413–421.

Franzke, A., German, D., Al-Shehbaz, I.A. and Mummenhoff, K. (2009) *Arabidopsis* family ties: molecular phylogeny and age estimates in Brassicaceae. *Taxon*, **58**, 425–437.

Geiser, C., Mandáková, T., Arrigo, N., Lysak, M.A. and Parisod, C. (2016) Repeated whole-genome duplication, karyotype reshuffling and biased retention of stress-responding genes in Buckler Mustards. *Plant Cell*, **28**, 17–27.

German, D.A. and Friesen, N.W. (2014) *Shehbazia* (*Shehbazieae*, Cruciferae), a new monotypic genus and tribe of hybrid origin from Tibet. *Turczaninowia*, **17**, 17–23.

Guerrero, R.F. and Kirkpatrick, M. (2014) Local adaptation and the evolution of chromosome fusions. *Evolution*, **68**, 2747–2756.

Guo, X., Liu, J., Hao, G. *et al.* (2017b) Plastome phylogeny and early diversification of Brassicaceae. *BMC Genomics*, **18**, 176.

Hohmann, N., Wolf, E.M., Lysak, M.A. and Koch, M.A. (2015) A time-calibrated roadm of Brassicaceae species radiation and evolutionary history. *Plant Cell*, **27**, 2770–2784.

Huang, D.I. and Cronk, Q.C.B. (2015) Plann: a command-line application for annotating plastome sequences. *Appl. Plant Sci.* **3**, apps.1500026.

Huang, C.H., Sun, R., Hu, Y., Zeng, L., Zhang, N., Cai, L., Zhang, Q., Koch, M.A., Al-Shehbaz, I. and Edger, P.P. (2016) Resolution of Brassicaceae phylogeny usingnuclear genes uncovers nested radiations and supports convergent morphological evolution. *Mol. Biol. Evol.* **33**, 394–412.

International Brachypodium Initiative (2010) Genome sequencing and analysis of the model grass *Brachypodium distachyon*. *Nature*, **463**, 763.

Jang, T.S., Emadzade, K., Parker, J., Temsch, E.M., Leitch, A.R., Speta, F. and Weiss-Schneeweiss, H. (2013) Chromosomal diversification and karyotype evolution of diploids in the cytologically diverse genus *Prospero* (Hyacinthaceae). *BMC Evol. Biol.* **13**, 136.

Kearse, M., Moir, R., Wilson, A., Stoneshavas, S., Cheung, M., Sturrock, S., Buxton, S., Cooper, A., Markowitz, S. and Duran, C. (2012) Geneious Basic: an integrated and extendable desktop software platform for the organization and analysis of sequence data. *Bioinformatics*, **28**, 1647–1649.

Kocsis, E., Trus, B.L., Steer, C.J., Bisher, M.E. and Steven, A.C. (1991) Image averaging of flexible fibrous macromolecules: the clathrin triskelion has an elastic proximal segment. *J. Struct. Biol.* **107**, 6–14.

Kougioumoutzis, K., Valli, A.T., Georgopoulou, E., Simaiakis, S.M., Triantis, K.A. and Trigas, P. (2016) Network biogeography of a complex island system: the Aegean Archipelago revisited. *J. Biogeogr.* **44**, 651–660.

Lanfear, R., Calcott, B., Ho, S.Y. and Guindon, S. (2012) Partitionfinder: combined selection of partitioning schemes and substitution models for phylogenetic analyses. *Mol. Biol. Evol.* **29**, 1695–1701.

Laslett, D. and Canback, B. (2004) ARAGORN, a program to detect tRNA genes and tmRNA genes in nucleotide sequences. *Nucleic Acid. Res.* **32**, 11.

Li, W., Challa, G.S., Zhu, H. and Wei, W. (2016) Recurrence of chromosome rearrangements and reuse of DNA breakpoints in the evolution of the Triticeae genomes. *G3*, **6**, 3837–3847.

Löytynoja, A. and Goldman, N. (2008) Phylogeny-aware gap placement prevents errors in sequence alignment and evolutionary analysis. *Science*, **320**, 1632–1635.

Luo, M.C., Deal, K.R., Akhunov, E.D. *et al.* (2009) Genome comparisons reveal a dominant mechanism of chromosome number reduction in grasses and accelerated genome evolution in Triticeae. *Proc. Natl Acad. Sci. USA*, **106**, 15780–15785.

Lysak, M.A., Berr, A., Pecinka, A., Schmidt, R., McBreen, K. and Schubert, I. (2006) Mechanisms of chromosome number reduction in *Arabidopsis thaliana* and related Brassicaceae species. *Proc. Natl Acad. Sci. USA*, **103**, 5224–5229.

Lysak, M.A., Cheung, K., Kitschke, M. and Bures, P. (2007) Ancestral chromosomal blocks are triplicated in Brassiceae species with varying chromosome number and genome size. *Plant Physiol.* **145**, 402–410.

Lysak, M.A., Mandáková, T. and Schranz, M.E. (2016) Comparative paleogenomics of crucifers: ancestral genomic blocks revisited. *Curr. Opin. Plant Biol.* **30**, 108–115.

Mandáková, T. and Lysak, M.A. (2008) Chromosomal phylogeny and karyotype evolution in x = 7 crucifer species (Brassicaceae). *Plant Cell*, **20**, 2559–2570.

Mandáková, T. and Lysak, M.A. (2016) Painting of Arabidopsis chromosomes with chromosome-specific BAC clones. *Curr. Protocols Plant Biol.* **1**, 359–371.

Mandáková, T. and Lysak, M.A. (2018) Post-polyploid diploidization and diversification through dysploid changes. *Curr. Opin. Plant Biol.* **42**, 55–65.

Mandáková, T., Joly, S., Krzywinski, M., Mummenhoff, K. and Lysak, M.A. (2010a) Fast diploidization in close mesopolyploid relatives of *Arabidopsis*. *Plant Cell*, **22**, 2277–2290.

Mandáková, T., Heenan, P.B. and Lysak, M.A. (2010b) Island species radiation and karyotypic stasis in *Pachycladon* allopolyploids. *BMC Evol. Biol.* **10**, 367.

Mandáková, T., Kovarík, A., Zozomová-Lihová, J., Shimizu-Inatsugi, R., Shimizu, K.K., Mummenhoff, K., Marhold, K. and Lysak, M.A. (2013) The more the merrier: recent hybridization and polyploidy in *Cardamine*. *Plant Cell*, **25**, 3280–3295.

Mandáková, T., Marhold, K. and Lysak, M.A. (2014) The widespread crucifer species *Cardamine flexuosa* is an allotetraploid with a conserved subgenomic structure. *New Phytol.* **201**, 982–992.

Mandáková, T., Li, Z., Barker, M.S. and Lysak, M.A. (2017a) Diverse genome organization following 13 independent mesopolyploid events in Brassicaceae contrasts with convergent patterns of gene retention. *Plant J.* **91**, 3–21.

Mandáková, T., Pouch, M., Harmanová, K., Zhan, S.H., Mayrose, I. and Lysak, M.A. (2017b) Multispeed genome diploidization and diversification after an ancient allopolyploidization. *Mol. Ecol.* **26**, 6445–6462.

Mohammadin, S., Peterse, K., van de Kerke, S.J. *et al.* (2017) Anatolian origins and diversification of *Aethionema*, the sister lineage of the core Brassicaceae. *Am. J. Bot.* **104**, 1042–1054.

Murat, F., Armero, A., Pont, C., Klopp, C. and Salse, J. (2017) Reconstructing the genome of the most recent common ancestor of flowering plants. *Nat. Genet.* **49**, 490–496.

Özüdoğru, B., Akaydın, G., Erik, S., Al-Shehbaz, I.A. and Mummenhoff, K. (2015) Phylogeny, diversification and biogeographic implications of the eastern Mediterranean endemic genus *Ricotia* (Brassicaceae). *Taxon*, **64**, 727–740.

Özüdoğru, B., Akaydın, G., Erik, S. and Mummenhoff, K. (2016) Seed morphology of *Ricotia* Brassicaceae and its phylogenetic and systematic implication. *Flora*, **222**, 60–67.

Özüdoğru, B., Al-Shehbaz, I. and Mummenhoff, K. (2017) Tribal assignment of *Heldreichia* Boiss. (Brassicaceae): evidence from nuclear ITS and plastidic *ndh*F markers. *Plant Syst. Evol.* **303**, 329–335.

Rannala, B. and Yang, Z. (2007) Inferring speciation times under an episodic molecular clock. *Syst. Biol.* **56**, 453–466.

Reis, M.D., Zhu, T. and Yang, Z. (2014) The impact of the rate prior on Bayesian estimation of divergence times with multiple loci. *Syst. Biol.* **63**, 555–565.

Renny-Byfield, S., Kovarik, A., Kelly, L.J., Macas, J., Novak, P., Chase, M.W., Nichols, R.A., Pancholi, M.R., Grandbastien, M.A. and Leitch, A.R. (2013) Diploidization and genome size change in allopolyploids is associated with differential dynamics of low- and high-copy sequences. *Plant J.* **74**, 829–839.

Robertson, W.R.B. (1916) Chromosome studies. I. Taxonomic relationships shown in the chromosomes of Tettigidae and Acrididae: V-shaped chromosomes and their significance in Acrididae, Locustidae, and Gryllidae: chromosomes and variation. *J. Morphol.* **27**, 179–331.

Schranz, M.E., Lysak, M.A. and Mitchell-Olds, T. (2006) The ABC's of comparative genomics in the Brassicaceae: building blocks of crucifer genomes. *Trends Plant Sci.* **11**, 535–542.

Sfenthourakis, S. and Triantis, K.A. (2017) The Aegean archipelago: a natural laboratory of evolution, ecology and civilisations. *J. Biol. Res. (Thessaloniki)*, **24**, 4.

Soltis, D.E., Visger, C.J., Marchant, D.B. and Soltis, P.S. (2016) Polyploidy: pitfalls and paths to a paradigm. *Am. J. Bot.* **103**, 1146–1166.

Stamatakis, A. (2014) RAxML version 8: a tool for phylogenetic analysis and post-analysis of large phylogenies. *Bioinformatics*, **30**, 1312–1313.

Stankiewicz, P. (2016) One pedigree we all may have come from – did Adam and Eve have the chromosome 2 fusion? *Mol. Cytogenet.* **26**, 72.

Wendel, J.F. (2015) The wondrous cycles of polyploidy in plants. *Am. J. Bot.* **102**, 1753–1756.

White, M.J.D. (1978) *Modes of Speciation*. San Francisco, CA: W. H. Freeman & Company.

Winterfeld, G., Becher, H., Voshell, S., Hilu, K. and Röser, M. (2018) Karyotype evolution in *Phalaris* (Poaceae): the role of reductional dysploidy, polyploidy and chromosome alteration in a wide-spread and diverse genus. *PLoS ONE*, **13**, e0192869.

Xiong, Z., Gaeta, R.T. and Pires, J.C. (2011) Homoeologous shuffling and chromosome compensation maintain genome balance in resynthesized allopolyploid *Brassica napus*. *Proc. Natl Acad. Sci. USA*, **108**, 7908–7913.

Yang, Z. (2007) PAML 4: phylogenetic analysis by maximum likelihood. *Mol. Biol. Evol.* **24**, 1586–1591.

Yang, L., Koo, D.H., Li, D. *et al.* (2014) Next-generation sequencing, FISH mapping and synteny-based modeling reveal mechanisms of decreasing dysploidy in *Cucumis*. *Plant J.* **77**, 16–30.

Zerbino, D.R. and Birney, E. (2008) Velvet: algorithms for de novo short read assembly using de Bruijn graphs. *Genome Res.* **18**, 821–829.